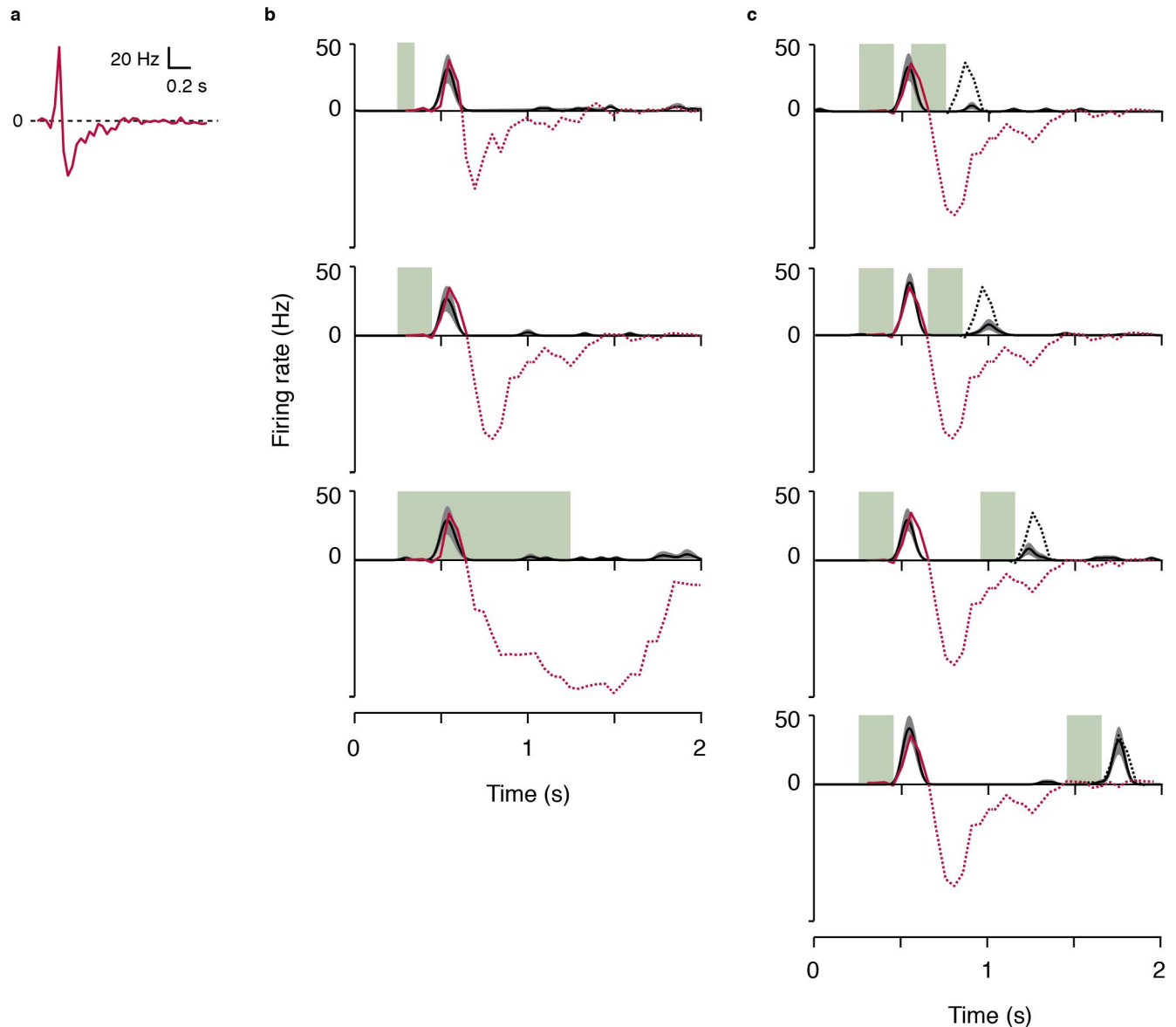


Supplementary Figure 1

Odor delivery system and basic characterization of odor output.

a. Photo-ionization detector (PID) output profile for a 500 ms pulse of Isoamyl Acetate (1% saturation). Vertical green bar marks odor ON period. Black line shows average response (12 trials, sampling rate 320 Hz). Grey band shows one standard deviation. Dashed red and green lines indicate time taken to reach 20% and 80% of the mean odor amplitude respectively. Dead time (grey) is the time taken from valve opening to reach 20% of mean. Rise time (pink) and decay time (blue) are the time taken to reach from 20% to 80% of mean amplitude and vice versa respectively.

b. Dead time, rise time and decay time for Isoamyl Acetate (IAA), Cineole (CIN), Limonene (LIM) and Methyl Amyl Ketone (MAK) at 1% saturation. Error bars indicate one standard deviation (pulse duration 500 ms, 20 repeats).



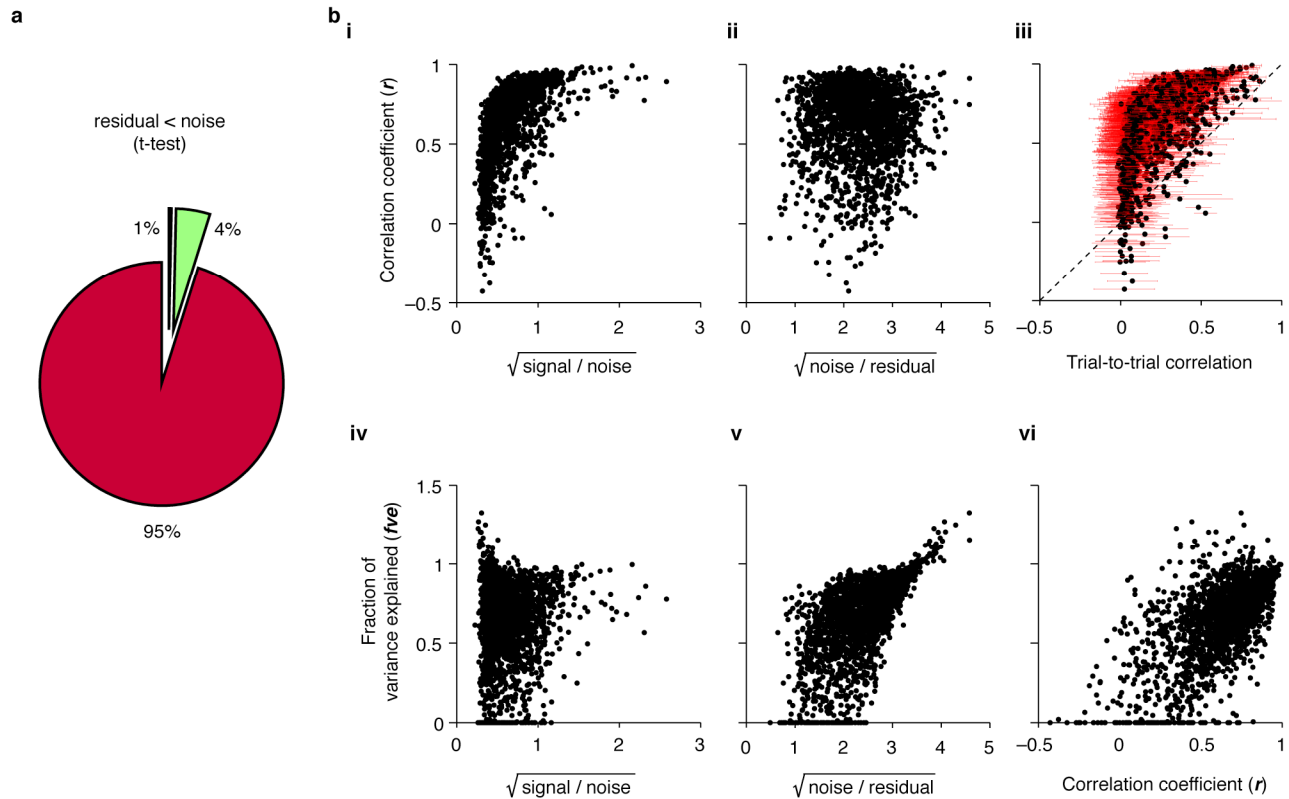
Supplementary Figure 2

Estimating inhibition from temporal summation of odor-evoked responses.

a. Estimated response kernel of an M/T cell for Isoamyl Acetate (IAA, 1% saturation).

b. Observed and predicted response of the cell in **a** to individual pulses of IAA. Vertical green bars indicate odor ON periods. Black lines show experimentally observed, average firing rate response across 12 trials. Grey bands indicate standard error of mean. Solid red lines show rectified, predicted firing rate response. Dotted red lines show negative firing rates (odor-evoked inhibition) estimated by the model. Pulse durations from top to bottom: 100, 200, 1,000 ms.

c. Response of the cell in **a** and **b** to paired odor pulses of IAA with variable inter-pulse durations. Solid black lines show experimentally observed average firing rate across 12 trials. Grey bands indicate standard error of mean. Red lines shows predicted firing rate in response to the first odor pulse alone. Dotted red lines show the unrectified, predicted inhibition evoked by the first odor pulse. Dotted black line represents the expected firing rate upon presentation of the second odor pulse, when presented in the absence of the first pulse. Inter-pulse durations from top to bottom: 200, 500, 1,000 ms. Individual pulse durations: 200 ms.



Supplementary Figure 3

Comparison of different descriptors of prediction quality for M/T cell responses to time-varying inputs of individual odors.

a. Summary pie-chart showing relative proportions of cell-stimulus pairs for which the residual error between the model prediction and experimentally observed mean firing rate response was significantly smaller than (red), equal to (green) or larger than (black) the observed trial-to-trial variability in the response (noise). Residuals included in this analysis were obtained from cross-validation procedures.

b. Comparison of different descriptors of prediction quality. All descriptors shown in this analysis were obtained from cross-validation procedures. 2,062 stimulus patterns, 130 M/T cells, 9 odors.

b(i). Distribution of correlation coefficient (r) between the model prediction and experimentally observed mean firing rate response across all cell-stimulus pairs as a function of signal-to-noise ratio in the experimentally observed responses.

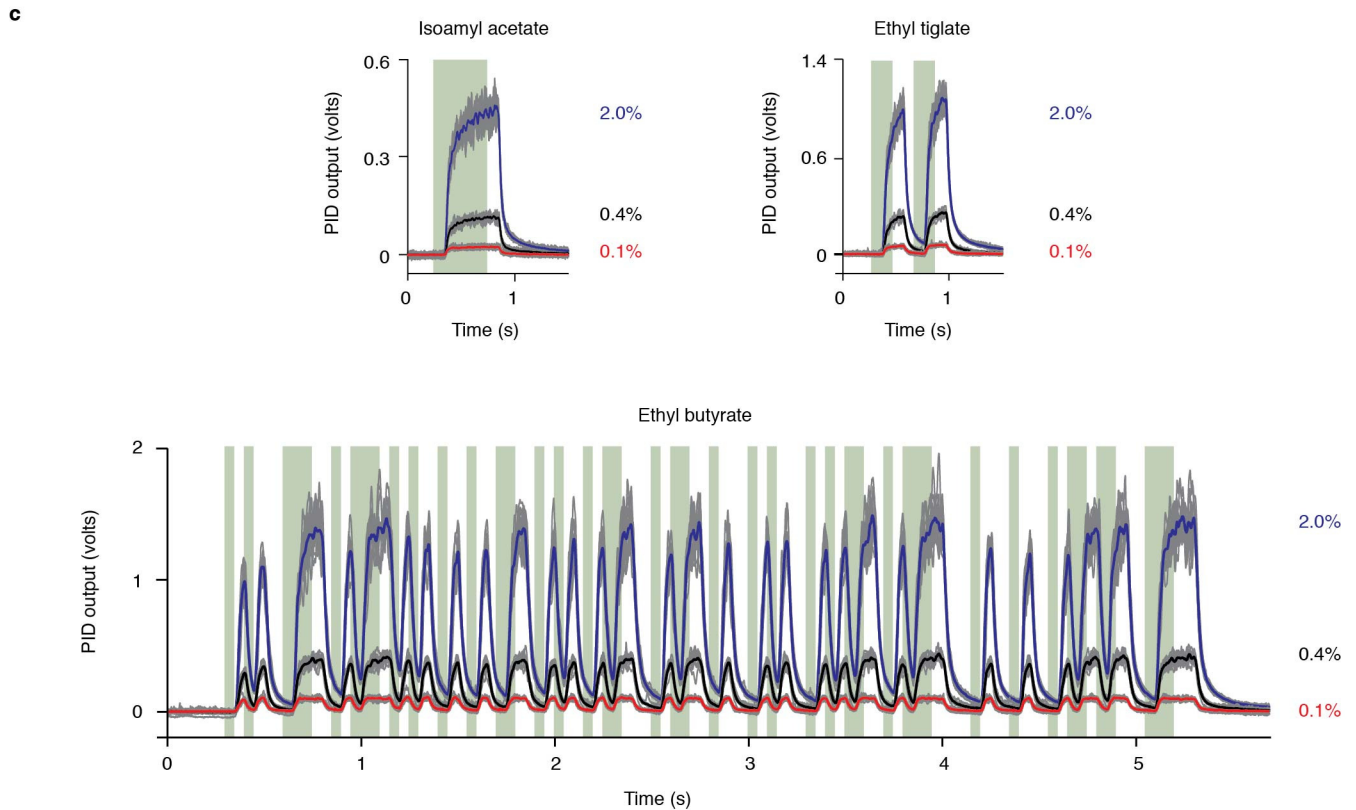
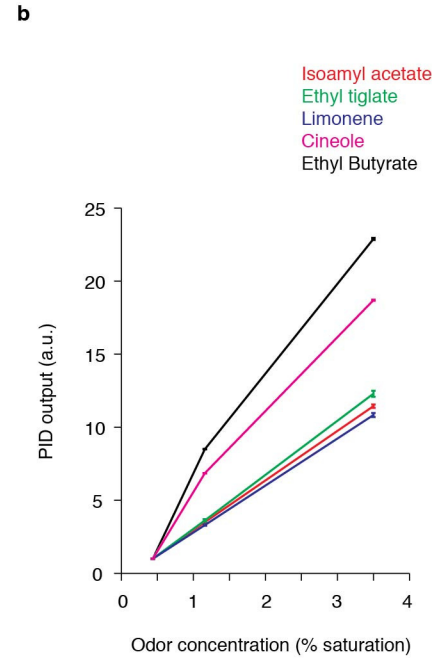
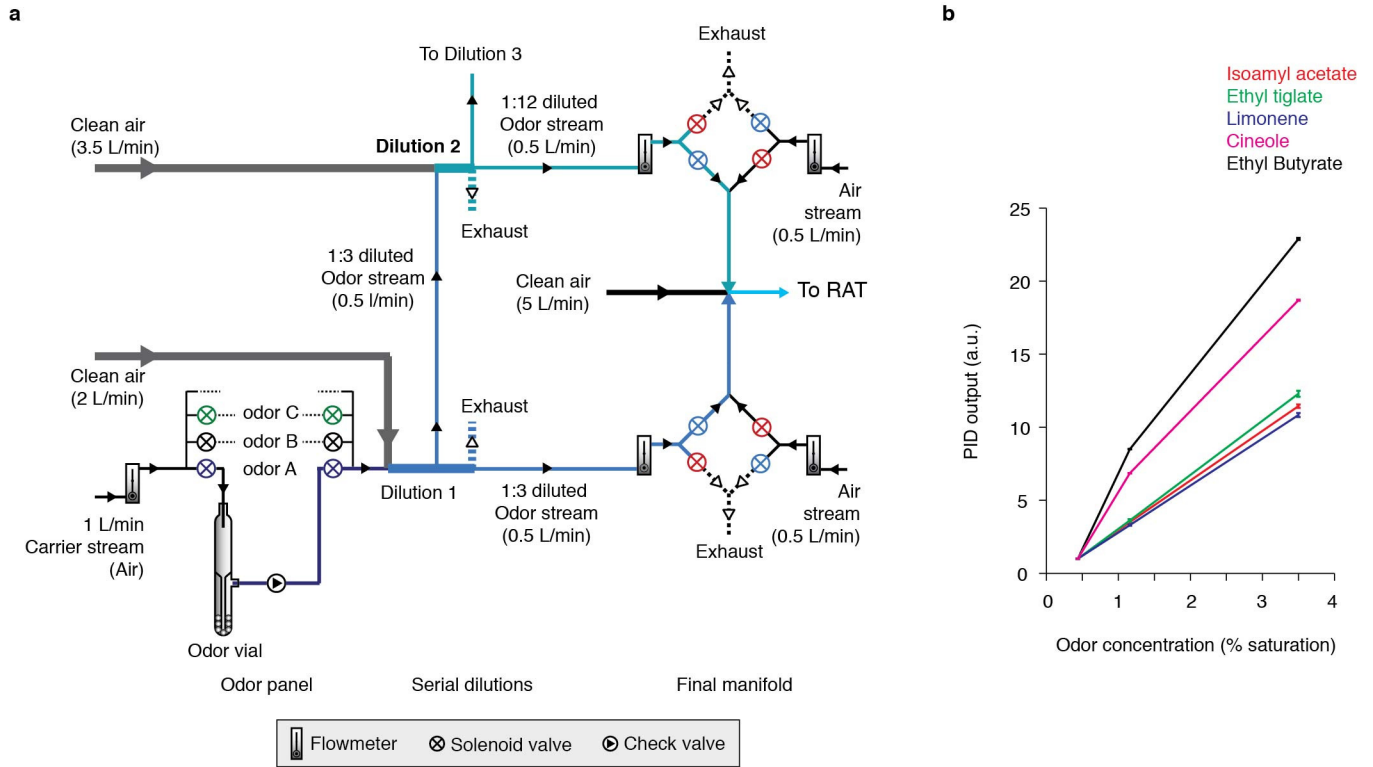
b(ii). Distribution of correlation coefficient (r) between the model prediction and experimentally observed mean firing rate response across all cell-stimulus pairs as a function of noise-to-residual ratio between the predicted and observed response.

b(iii). Distribution of correlation coefficient (r) between the model prediction and experimentally observed mean firing rate response across all cell-stimulus pairs as a function of average pair-wise correlation across trials for a given stimulus. Each dot represents one stimulus. Red lines indicate the standard deviation of the pair-wise average trial-to-trial correlation across all possible pairs of trials. Points lying above the slope of unity (dotted black line) indicate that correlation of predicted response to the mean is greater than the trial-to-trial correlation in the response.

b(iv). Distribution of the fraction of variance explained (fve) by the model across all cell-stimulus pairs as a function of signal-to-noise ratio in the experimentally observed responses.

b(v). Distribution of the fraction of variance explained (fve) by the model across all cell-stimulus pairs as a function of noise-to-residual ratio between the predicted and observed response.

b(vi). Distribution of the fraction of variance explained (fve) by the model across all cell-stimulus pairs as a function of the correlation coefficient (r) between the model prediction and experimentally observed mean firing rate response across all cell-stimulus pairs.



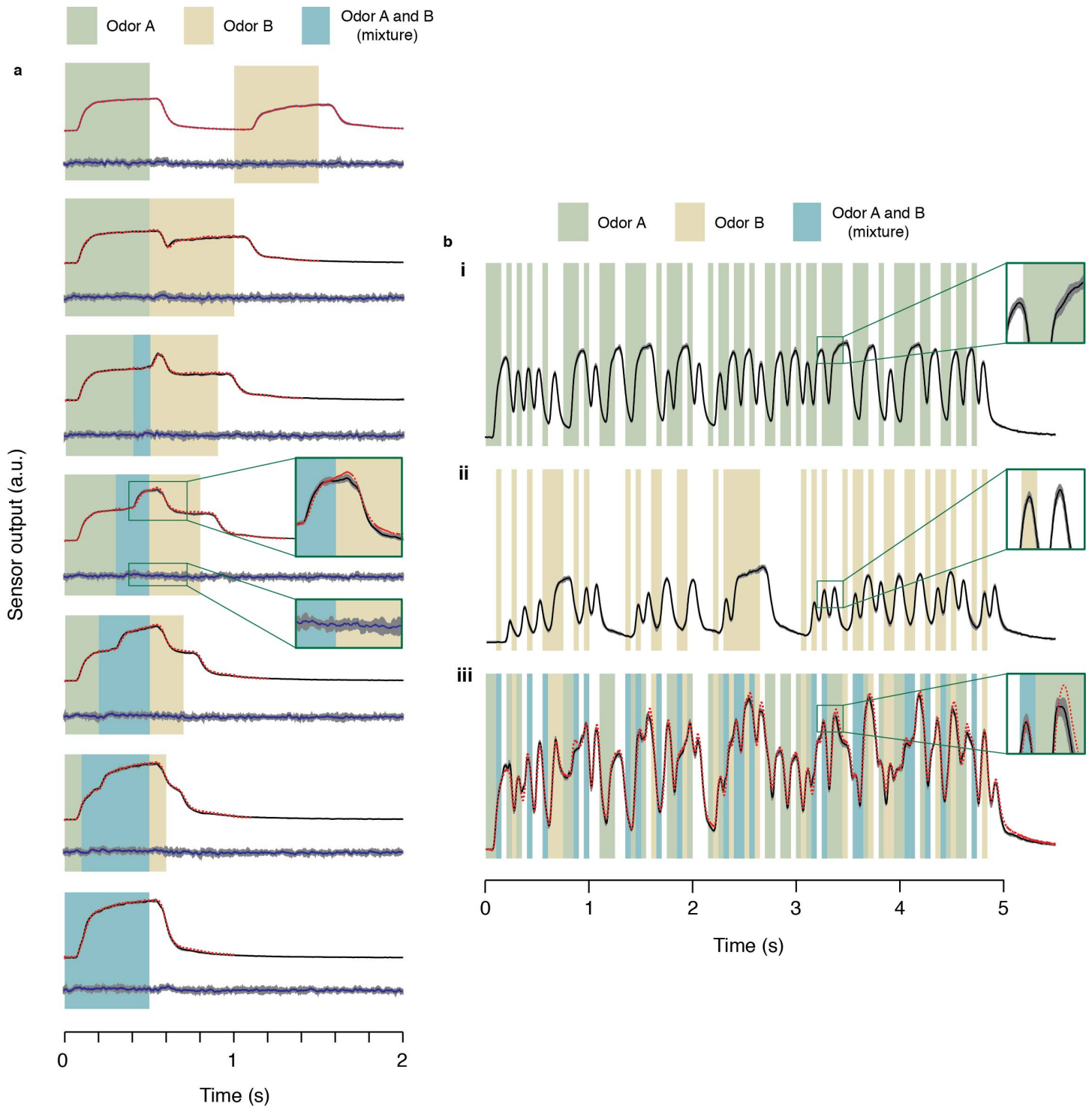
Supplementary Figure 4

Linear concentration control across chemically diverse odors with random interleaving of multiple concentrations.

a. Schematic of the odor delivery system for reliable and linear concentration control. Saturated odor stream, produced by bubbling the carrier air stream through a selected vial (e.g. Odor A) in the Odor panel is diluted with a 2 L/min clean air stream to obtain 1:3 dilution. One fraction of this 1:3 diluted odor stream is routed to the final manifold at a regulated flow rate (0.5 L/min) where it is further diluted 10-fold by a high-flow rate carrier stream (5 L/min) and switched between Rat and Exhaust by two pairs of anti-coupled solenoid valves (similar to that described in **Fig. 1a**). This results in a final output concentration of 3.5% saturation at the animal's snout. Lower concentrations of the same odor are obtained by setting up additional serial dilutions of the initial 1:3 diluted odor stream before the final manifold. For example, a second fraction of the 1:3 diluted stream is mixed with 3.5 L/min clean air to obtain a net dilution of 1:12 instead of the original 1:3 dilution. This 1:12 dilution stream is also routed to the final manifold at a regulated flow rate (0.5 L/min) and switched between Rat and Exhaust by the same mechanism as that described for the 1:3 diluted stream. As a result, the net output concentration of this stream is 4 times lower than the first stream. Even lower concentrations can be obtained by setting up as many serial dilutions, as required, of the original 1:3 diluted stream. Linearity of the concentration output in this design is conferred by the use of a common step for creating 100% saturated vapor of the odor and modulating concentration only via serial dilutions of the odorized air. The ability to interleave different concentrations is conferred by the fully independent control of each concentration stream at the final manifold. Since the different concentrations do not share any common valves, there is no cross-contamination and low concentration stimuli can be delivered in quick succession to high concentration ones without spillover across trials.

b. Linear odor output across five chemically diverse odors measured as the average photo-ionization detector (PID) response amplitude within a 500 ms odor pulse. Average PID amplitude was calculated from 12 trials across randomly interleaved presentations of three different concentrations. Error bars indicate one standard deviation.

c. Observed output profile for three odors (Isoamyl acetate, Ethyl tiglate and Ethyl butyrate) for stimulus patterns delivered at three different concentrations (0.1%, 0.4% and 2% saturation). Vertical green bars mark odor valve ON periods. Red, black and blue lines show average response amplitude of a PID (sampling rate 1KHz) across 12 trials at three different concentrations (0.1%, 0.4% and 2%) from a set of randomly interleaved trials of all three concentrations. Grey lines show individual trials. Note that the relative difference in amplitude across the three concentrations for each odor is similar despite the differences in PID sensitivity for each odor.



Supplementary Figure 5

Output odor characteristics for binary odor stimuli.

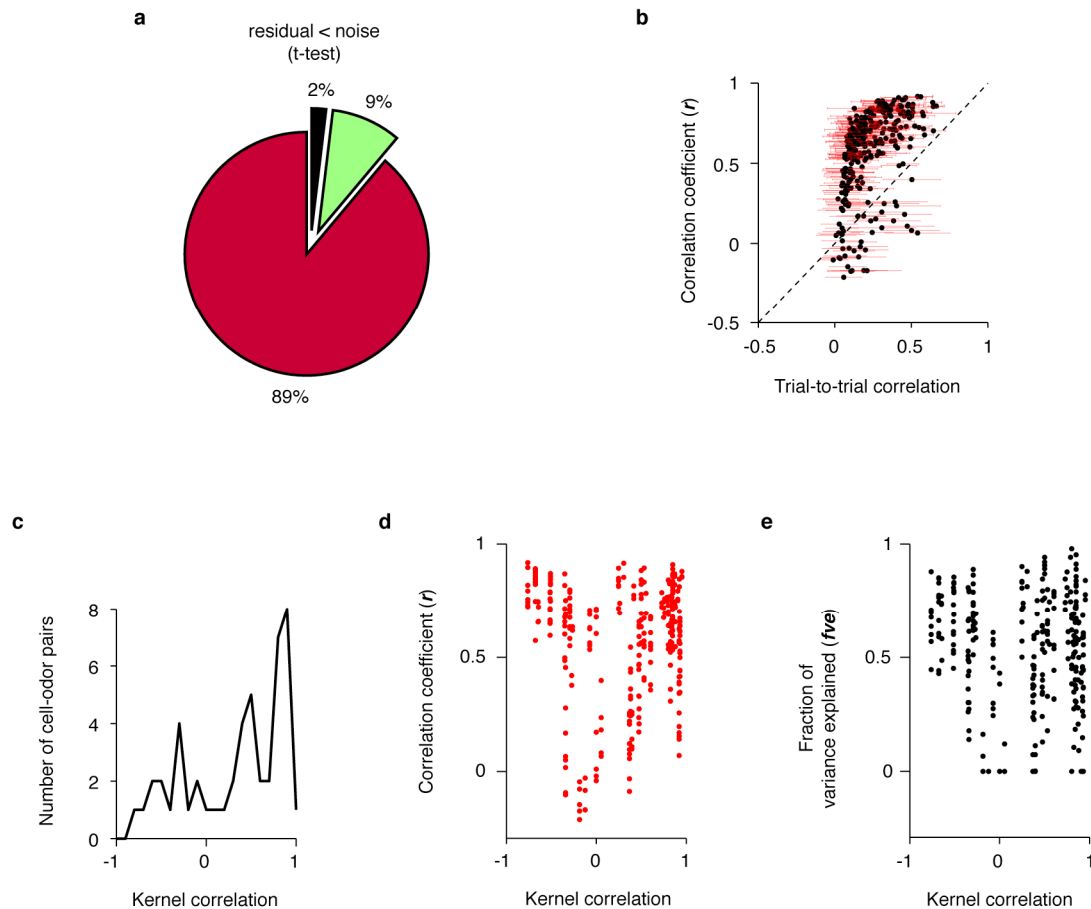
a. PID and anemometer output profile for pairs of odor pulses of Isoamyl Acetate (IAA, 1% saturation) and Limonene (LIM, 1% saturation) at varying inter-pulse intervals. Vertical green, yellow and cyan bars represent odor ON periods for IAA, LIM, or both, respectively. Black and blue lines show simultaneously measured, average PID and anemometer response respectively. Grey bands indicate one standard deviation (10 trials). Dotted red lines show the expected PID output, calculated as a sum of the measured PID

outputs for individual pulses of each odor. Inter-pulse intervals from top to bottom (in ms): 1,000 (no overlap), 500, 400, 300, 200, 100 and zero (complete overlap); individual pulse durations: 500 ms.

b. PID output profile for pseudo random fluctuating patterns of two odors presented simultaneously.

B(i,ii). Black lines show average PID output for a fluctuating pattern of Limonene (LIM, 1% saturation) and Cineole (CIN, 1% saturation) respectively.

b(iii). Black and dotted red lines show observed and expected PID response upon simultaneous presentation of the patterns in **b(i)** and **b(ii)**. Grey bands indicate one standard deviation (10 trials each). Vertical green, yellow and cyan bars represent odor ON periods for LIM, CIN, or both, respectively.



Supplementary Figure 6

Assessment of prediction quality for M/T cell responses to binary odor mixtures as a function of response variability and similarity of kernels across the two component odors.

a. Summary pie-chart showing relative proportions of cell-stimulus pairs for which the residual error between the model prediction and experimentally observed mean firing rate response was significantly smaller than (red), equal to (green) or larger than (black) the observed trial-to-trial variability in the response (noise). 314 stimulus patterns, 48 M/T cell-mixture pairs.

b. Distribution of correlation coefficient (r) between the model prediction and experimentally observed mean firing rate response across all cell-stimulus pairs as a function of average pair-wise correlation across trials for a given stimulus. Each dot represents one stimulus. Red lines indicate the standard deviation of the pair-wise average trial-to-trial correlation across all possible pairs of trials. Points lying above the slope of unity (dotted black line) indicate that correlation of predicted response to the mean is greater than the trial-to-trial correlation in the response.

c. Distribution of correlation coefficient between the kernels for each of the two odors composing the binary mixture, across all odor pairs in the mixture dataset (48 cell-mixture pairs).

d. Distribution of correlation coefficient (r) between the model prediction and experimentally observed mean firing rate response across all cell-stimulus pairs as a function of correlation between the kernels for each of the two odors composing the binary mixture stimulus.

e. Distribution of the fraction of variance explained (fve) by the model across all cell-stimulus pairs as a function of correlation between the kernels for each of the two odors composing the binary mixture stimulus.